BEARING LOAD ANALYSIS OF RECIPROCATING PISTON COMPRESSORS

Bernhard Fritz
Recip Service Compressor Expert
Hoerbiger Wien GmbH
Vienna, Austria

Alessandro Baldussu
Engineering Manager RU Service Europe
Hoerbiger Benelux B.V
Heerlen, Netherlands

Andreas Brandl
Global Engineering Manager Compression Service
Hoerbiger Wien GmbH
Vienna, Austria

Bernhard Fritz studied Mechanical Engineering at the Technical University of Vienna and obtained his Ph.D. at its Institute of Fluid Mechanics and Heat Transfer 2019. He joined the HOERBIGER Research and Development (R&D) department in 2012. Within the R&D department, he was leading the Advanced Simulation Group, supporting various projects of R&D and Product Management. Since 2021 he is part of the global HOERBIGER Service Engineering team and works closely with the local entities, providing his expertise in advanced engineering and simulation methods.

Alessandro Baldussu studied Mechanical Engineering at the Università degli Studi di Firenze and obtained his Ph.D. from Politecnico di Milano and Technische Universität München in 2014. He worked in the Recip engineering department of Nuovo Pignone until July 2020. After this experience he joined HOERIGER in the role of Engineering manager for the Regional Unit Service Europe. The main tasks on his role, aside the lead of engineering team of the Benelux branch, are RCA, Design of Capital Parts and Solutions proposal for Recip Upgrades.

Andreas Brandl is the Engineering Manager at HOERBIGER for Compression Service in Vienna. His work focuses on Reciprocating Compressors for the energy and chemical industry. Before is current assignment, Andreas has had several other roles within HOERBIGER such as R&D engineering and Engineering management in USA. Andreas earned his Master's degree in mechanical engineering at the Vienna University of Technology and his MBA at the Jones Graduate School of Business at Rice University.

ABSTRACT

Many problems in today's industrial environment require smart modeling assumptions in order to make them numerically accessible with an acceptable amount of effort. This case study shows how a field problem (main bearing failures) is turned into a numerical model: we present a bearing force analysis of a 5-throw reciprocating compressor with severe problems on its third main bearing. Inertial and gas-dependent forces are calculated. The crankshaft is modeled as a uniform beam; its load-dependent deformation and the resulting bearing loads are estimated based on Clapeyron's three-moment equation with the assumption of zero bearing clearances. The resulting calculation time is < 1s for a 360-degree load cycle, allowing detailed studies that yield conclusive results: polar load diagrams clearly confirm that the problematic bearing is exposed to the highest loads in operation. The short calculation time allows for parametric studies investigating the effect of lower reciprocating masses, partial load conditions, counterweights, different crankshaft designs, or combinations of the above.

INTRODUCTION

An operator has eight reciprocating piston compressors, all identical in design. These have repeatedly suffered from bearing problems: although the lifetime of the critical bearings has decreased over the years (probably correlated with increasing machine vibrations and wear of components such as bearing caps), the lifetime of the bearings has never been satisfactory from the beginning. In particular, the third main bearing (numbered from the drive side) has always caused trouble, with run times never exceeding 12 months. It was therefore decided that a detailed evaluation of the bearing loads would yield ideas on how to lengthen the service interval beyond what can be achieved by regular repair measures like reboring the crankcase and repairing the crankshaft and bearing shells. In the course of this work, possible ways to reduce the load on individual bearings were studied:

- reduce the piston weight to reduce bearing forces due to oscillating masses;
- introduce stepless capacity control: preferential unloading of certain cylinders (HE side and or CE side) might reduce the load on the critical bearing, with the penalty of reducing the overall delivery quantity;
- add counterweights to the crankshaft to balance the rotating mass forces;
- change the crank throw angles with the aim of better load balancing.

COMPRESSOR DESIGN

The compressor design is quite uncommon: it is a horizontally opposed five-throw machine in which the crank angles are arranged non-uniformly (Figure 1). It compresses natural gas from 32 bar to 63 bar (465 psi to 913 psi) in a single stage. Table 1 shows the most important specifications, and Table 2 shows the reciprocating and rotating masses. This is a low-speed machine, running at 375 rpm (5 m/s average piston speed) and with a bore of 250 mm (9.84 in).

Figure 2 and Table 3 show the crank angles: first throw at 0 degrees, second throw at 204.3 degrees, third throw at 155.6 degrees, fourth throw at 294.3 degrees, and fifth throw at 65.6 degrees. The non-uniform crank design allows an uneven number of throws and the placement of main bearings in between each throw. However, unlike boxer designs, there exist unbalanced mass forces which result in higher bearing loads and free foundation forces. In addition, the crankshaft that is installed in this machine does not include counterweights to minimize the rotating mass forces.

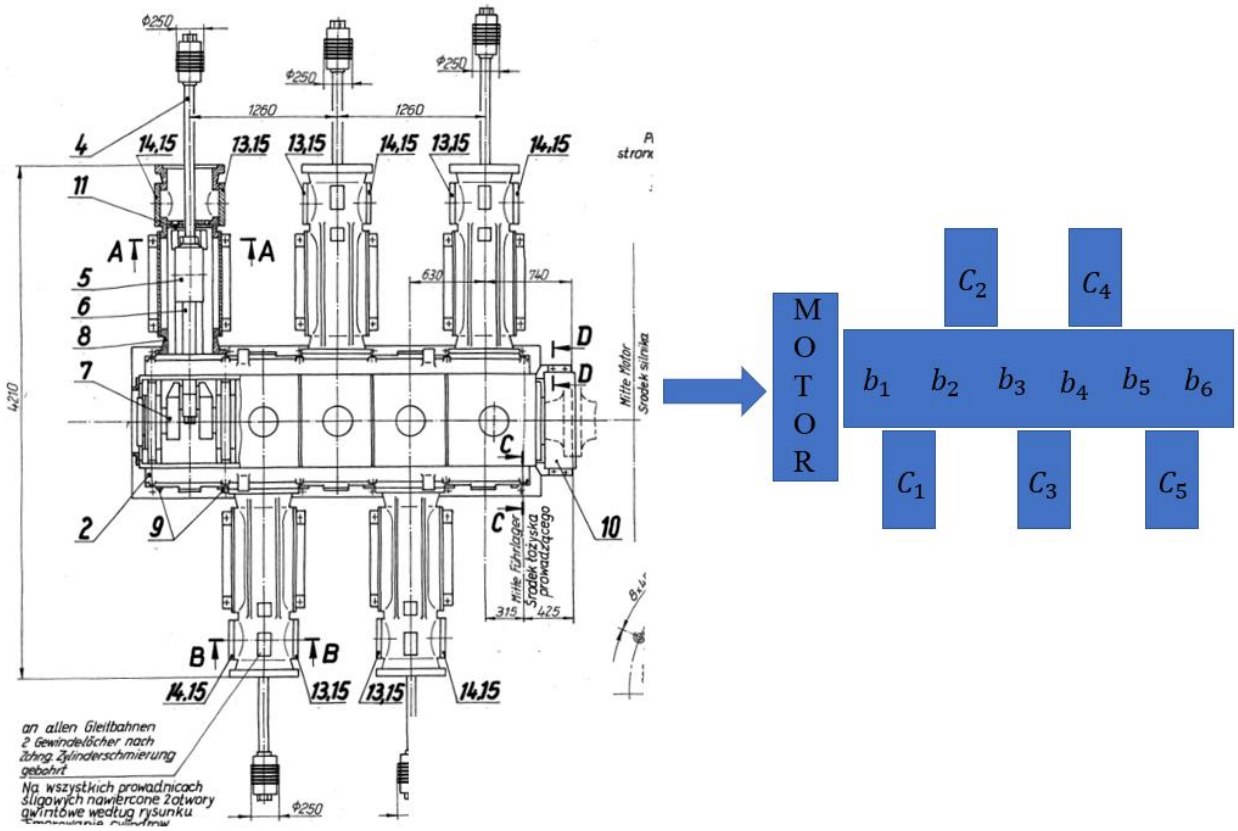

Figure 1: Cylinder arrangement and numbering system used in this paper

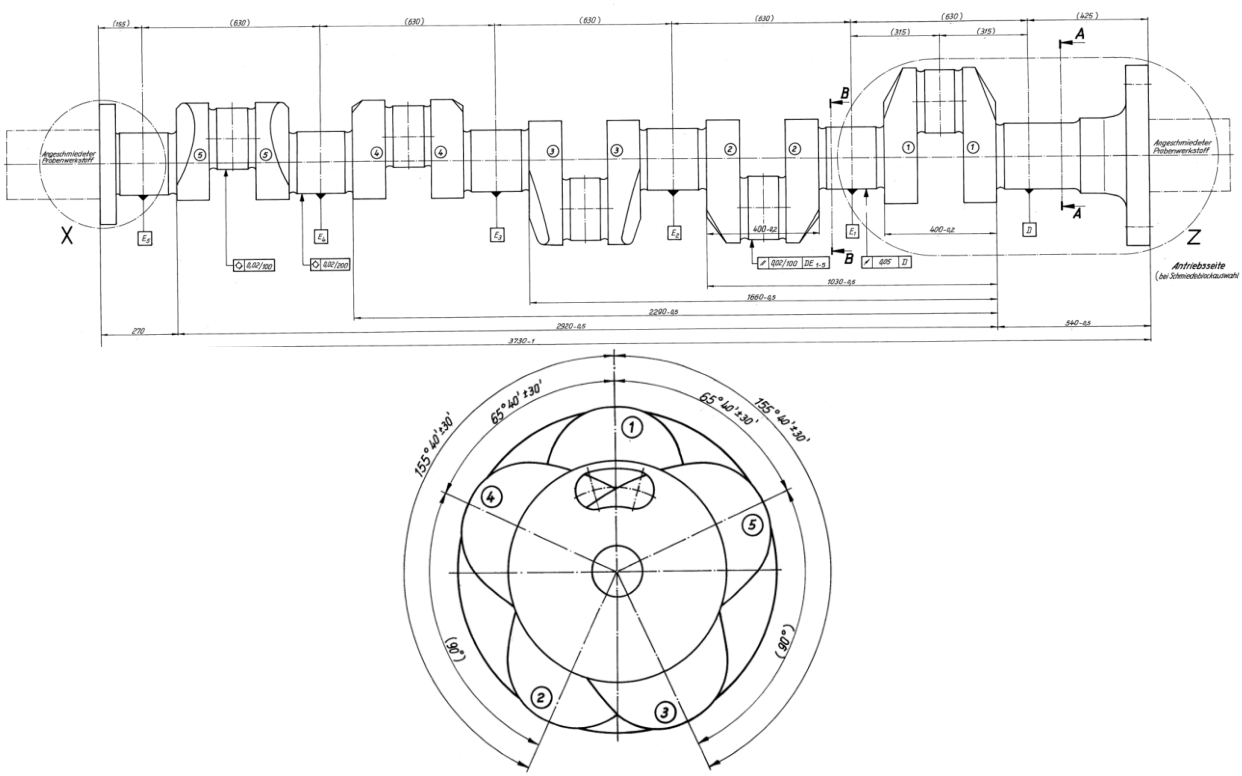

Figure 2: Crankshaft side view (top) and end view (bottom).

Table 1: Basic geometry and parameters of the compressor.

Compressor parameters	
Speed	375 rpm
Bore	250 mm
Stroke	400 mm
Average piston speed	5 m/s
Suction pressure	31 bar
Discharge pressure	55 bar

Table 2: Relevant masses for inertia forces.

Part	Mass (kg)
Piston and piston rod	180
Crosshead	145
Connecting rod	178
Total reciprocating mass	384
Rotating mass	118

Table 3: Offset angles of the crankshaft.

Throw number	Offset angle (degrees)
1	0
2	204.3
3	155.6
4	294.3
5	65.6

Typical bearing failure patterns on this machine

The frictional layers of the main bearings are made out of a standard babbitt material. According to Wittel, et al. (2013), the maximum allowable specific bearing load (average surface pressure for the projected bearing area (diameter x axial width)) for Sn-Pb alloys is 5 MPa (725 PSI). This average surface pressure adds up to approx. 210kN (45,000 lbf) for the bearing design in use. Of course, this is only a rough guide, since the max. pressures within the bearings, which lead to fatigue failures, are much higher and are highly dependent on tilt, oil viscosity, clearances, vibrations, etc.

Figure 1 shows the numbering system: bearing no. one is the thrust bearing on the drive side, while number six is the last bearing, next to throw five.

Typical failure symptoms after approximately 700 hours of operation are shown in Figure 3 (all bearings) and Figure 4 (bearing no. 3). Bearings one to four show defects. On bearings one, two and four (b_1, b_2 and b_4) the failures are towards the edges, and most likely correlate with misalignments of the bearing bores relative to the crankshaft. For this study, however, we concentrate on bearing three (b_3), which shows clear signs of fatigue damage resulting from overloading. As we will show later, the area showing the most wear also experiences the highest stresses due to the alternating loads.

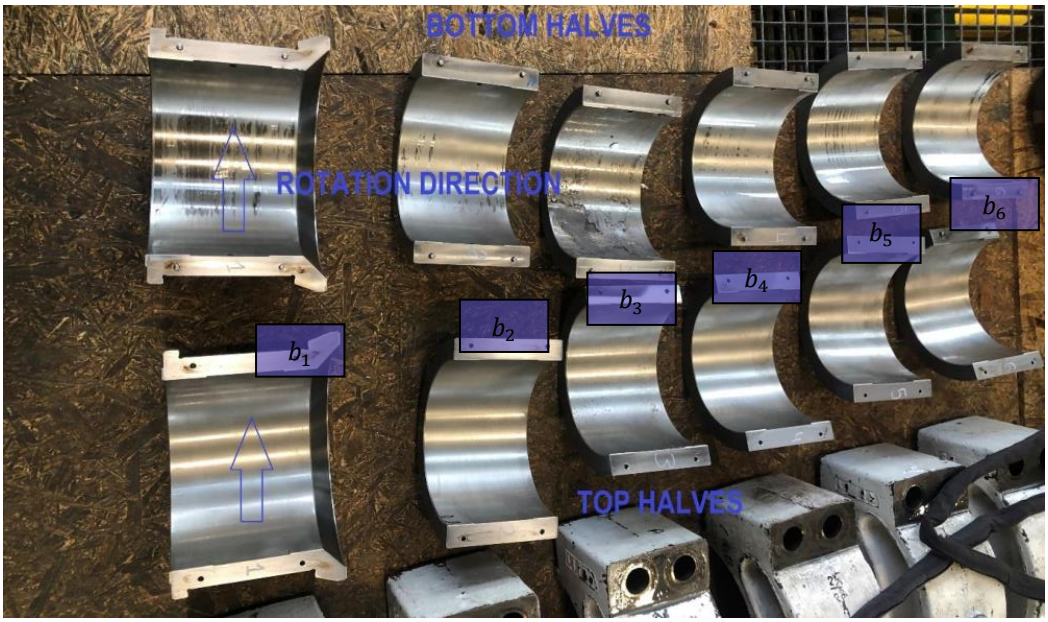

Figure 3: Running surfaces of the bearings after 700 h operation.

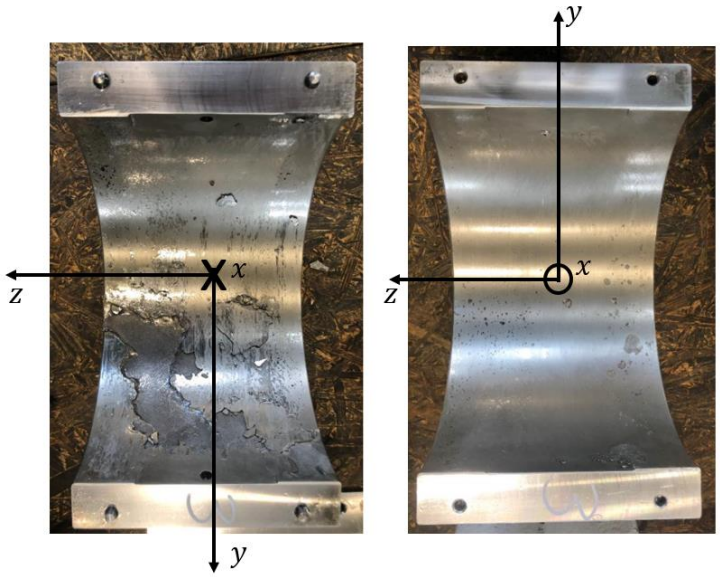

Figure 4: Bearing shells of bearing no. 3 (left: lower half, right: upper half) after 700 h operation. Note the coordinate system, which we use later in the simulations. The region of significant damage corresponds to the highest calculated loads.

APPROACH

To estimate how changing masses, capacity control systems and other potential modifications will affect the life of the bearings we need to derive the force F_{B_i} on each bearing. This is done by first calculating the throw forces F_{C_i} (Forces acting in direction of the piston rod at the location of the crosshead pin) and then in a second step deriving the bearing forces.

The piston motion and the throw forces, including inertial forces, are calculated in the standard way (e.g. Küttner, 2013). Throw forces are calculated assuming isentropic compression and expansion. The valves are assumed to open and close instantly, according to the differential pressure acting on them. The mass flow through each valve is estimated using the well-known Saint-Venant-Wantzel law, which describes the isentropic flow of an ideal gas out of a pressure vessel:

$$\dot{m} = A_1 \sqrt{\frac{2\kappa}{\kappa - 1} \rho_0 p_0} \sqrt{\left(\frac{p_1}{p_0}\right)^{\frac{2}{\kappa}} - \left(\frac{p_1}{p_0}\right)^{\frac{\kappa+1}{\kappa}}} \tag{1}$$

The index 0 denotes conditions within the vessel (hence, pressure in the cylinder or pulsation damper), while index 1 refers to the outside (the manifold).

In the second step we derive the forces acting on the bearings throughout the compressor cycle. This is done using the approach of Nikolic et al. 2012, which is summarized in the following paragraphs. The crankshaft is modelled as a statically indeterminate continuous beam. The beam is supported at the center positions of the bearings and carries the throw forces, which act at the center positions of the big-end bearings (Figure 5).

Each crank i produces a force F_{C_i} that is distributed to all the bearings b_j $(j = 1,2, \dots 6)$ as $F_{b_{ij}} = \rho_{ij} F_{C_i}$, where $\sum_{j=1}^{6} \rho_{ij} = 1$. The "influence coefficients" ρ_{ij} show to what extent the force F_{C_i} affects bearing b_j. Six influence coefficients can be derived for each bearing, yielding a 5×6 matrix. The influence coefficients for any continuous beam, regardless of the number of supports, can be calculated from the well-known Clapeyron three-moment equation, which is based on classical beam theory together with the principle of superposition. In this case we derive the matrix:

$$\rho = \begin{bmatrix} 0.40 & 0.73 & -0.16 & 0.04 & -0.01 & 0.00 \\ -0.07 & 0.57 & 0.61 & -0.13 & 0.03 & -0.01 \\ 0.02 & -0.12 & 0.60 & 0.60 & -0.12 & 0.02 \\ -0.01 & 0.03 & -0.13 & 0.61 & 0.57 & -0.07 \\ 0.00 & -0.01 & 0.04 & -0.16 & 0.73 & 0.40 \end{bmatrix} \tag{2}$$

Figure 6 shows typical results when we use these values of ρ to calculate the reaction forces and the (exaggerated) crankshaft deformation due to the forces on an individual throw, in this case F_{C_3} and F_{C_5}.

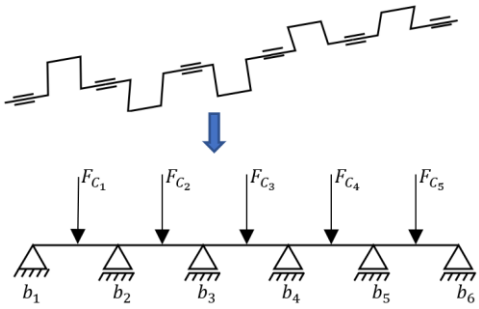

Figure 5: Mechanical model of a continuous beam with intermediate supports and bending forces.

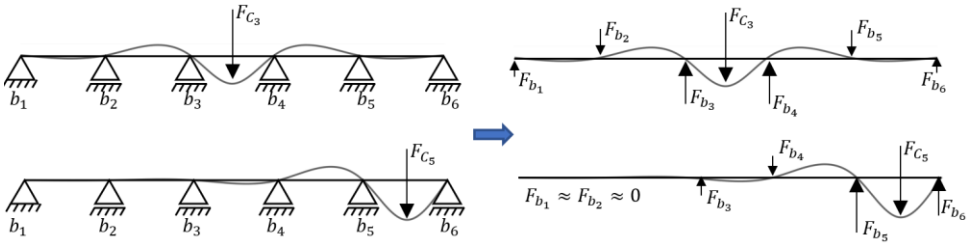

Figure 6: Distribution of bearing loads (and crankshaft deformation) due to a single crank force at throw 3 (top) or throw 5 (bottom), as calculated from the influence coefficients ρ shown in (2).

Having derived the coefficient matrix and the gas and inertial forces acting on each throw, we can calculate each bearing force F_{b_j} using the principle of superposition:

$$F_{b_k} = \sum_{j=1}^{5} F_{b_{jk}} = \sum_{j=1}^{5} \rho_{jk} F_{C_j} \tag{3}$$

Care must be taken to account for the fact that each throw i corresponds to a different offset angle φ_i, and that all the forces $F_{C_i}(\varphi_i)$ have different directions and magnitudes over time. Hence individual coordinate systems are used for each throw, each rotated around the axis of the crankshaft by its offset angle. The kinematic correlations are comprehensively described in Nikolic et al. 2012.

The numerical implementation is straight forward. For this specific case, the general-purpose programming language python (Van Rossum 1955) is used. Computational time is not of concern, results are derived within a second.

RESULTS

First, we studied the forces acting on each throw. Since all five throws are identical, these forces are the same as long as we do not use capacity control or change the masses of individual pistons or crossheads; they are just time-shifted according to the crank offset angles. Once we have calculated the throw forces, in a second step we can study the effects of the most promising configurations on the final bearing loads.

Throw forces

Figure 7 shows the forces on throw one (in its original configuration). We see that the inertia forces F_i and the gas forces F_g have the same order of magnitude, so in principle we could reduce the crank pin forces F_pin by reducing either F_i or F_g. This graph looks the same for all the throws as long as no parameters are changed, with the exception that the load curve of each throw is shifted by its offset angle. F_t and F_r denote the tangential and radial components, respectively, of F_pin.

The red crosses in Figure 7 mark local maxima of F_t and F_r. For throw one the maxima occur at approximately Θ = 30 degree, 72 degree, 218 degree and 262 degree. Table 4 shows the corresponding angles of the maxima for the pin forces in throws two and three, which are the critical ones for bearing three. To facilitate comparisons, the red crosses also appear on the polar diagrams below (Figure 10 etc.).

Table 4: Crank angles at which the pin forces F_t and F_r reach local maxima.

Throw number	Crank angles (degrees)
Throw 2	54, 96, 242, 286
Throw 3	185, 227, 8, 52

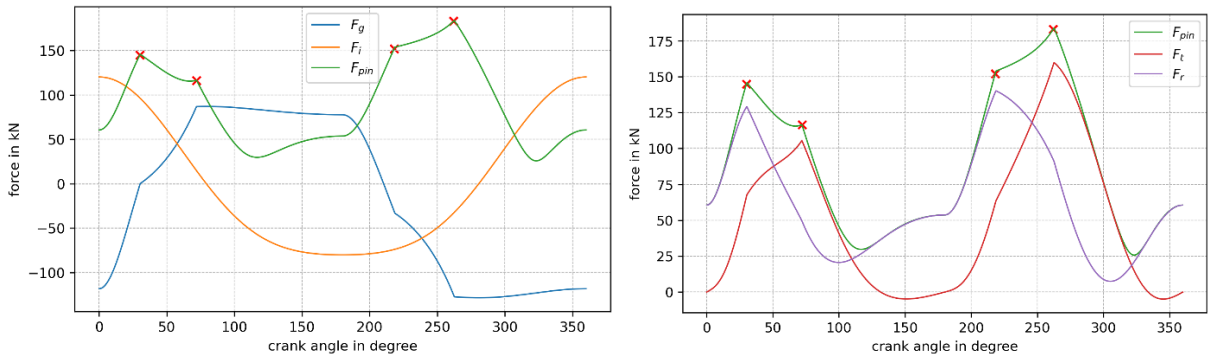

Figure 7: Forces acting on each throw at 100 percent load: F_g (blue) and F_i (orange) combine to create F_pin at the big-end bearing (left image). The right image shows F_rad and F_t components of F_pin.

The inertial forces can be reduced by reducing the reciprocating masses (either crosshead or piston masses). The operator has already implemented this measure, using pistons made from lower-density material to reduce the mass of the piston and piston rod assembly from 180 kg to 116 kg (397 lb to 256 lb). Figure 8 compares the pin forces produced by the heavy and light pistons: the light piston reduces the pin force by between zero and approximately 12 percent, depending on the crank angle. The effect of this reduction on the final bearing forces will be studied later.

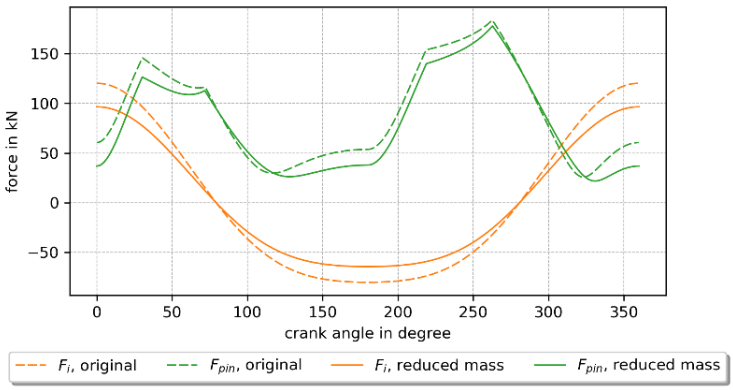

Figure 8: How piston weight affects the throw forces. The dashed lines refer to the original piston, while the solid lines show the forces developed using a lighter piston that reduces the mass of the piston and piston rod from 180 kg to 116 kg.

The other possibility to reduce the pin forces is to use a capacity control system that forces the discharge valve to stay open during part of the compression stroke. This is usually done to reduce the compressor's output without wasting energy, and it is important to check that the small-end bearing sees sufficient rod-load reversal to avoid oil starvation. In our case, however, it is also worth looking at how cylinder unloading affects the pin forces on the main bearing, and hence the bearing loads.

Figure 9 shows four different unloading strategies: completely idle (no compression in the cylinder); idling the head end (HE) of the double-acting cylinder; idling the crank end (CE); and 80 percent load on both HE and CE. Complete idling leads to a significant reduction in force for 220 degree < Θ < 300 degree, but also a significant increase for 310 degree < Θ < 25 degree. Idling the crank end is only beneficial for 180 degree < Θ < 300 degree, while idling the head end is only beneficial for 0 degree < Θ < 90 degree. A load strategy that combines the positive effects of those mentioned above is to run at 80 percent load at both ends: Figure 9 (bottom left) shows how this leads to a 20 percent reduction in F_{pin}.

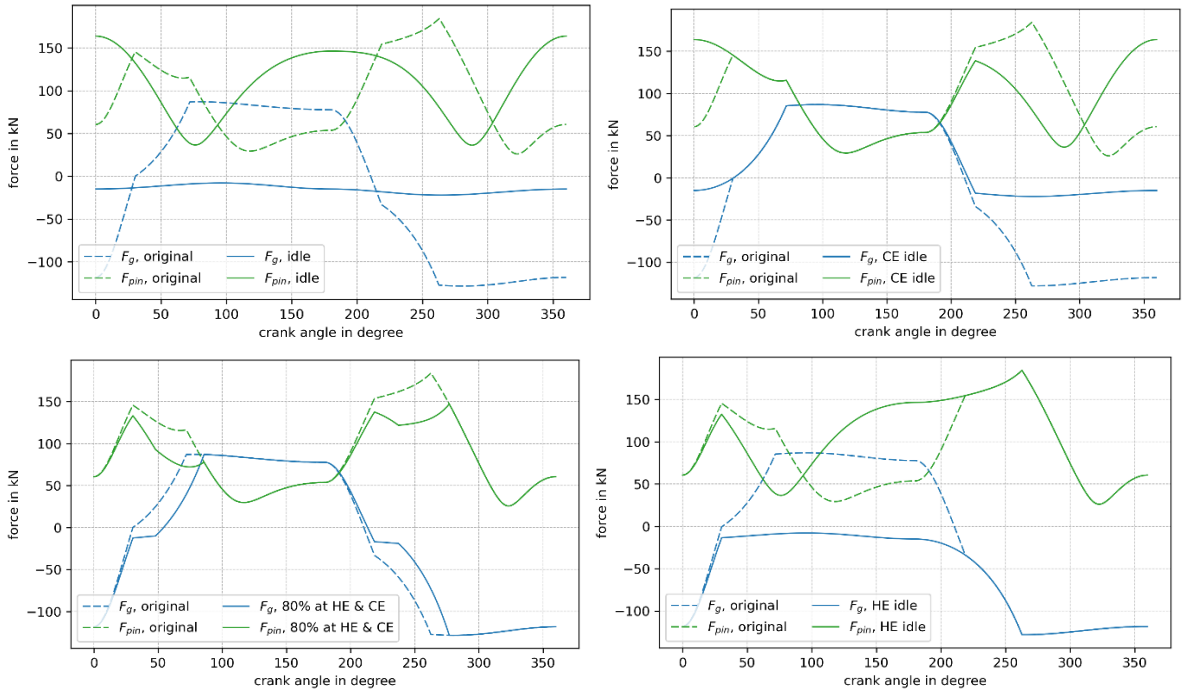

Figure 9: Throw forces for different capacity control arrangements: (top left) fully idle (no compression); (top right) idling the crank end of the cylinder; (bottom right) idling the head end of the cylinder; (bottom left) 80 percent capacity at both ends of the cylinder.

Now we have an idea of how to decrease the individual throw forces, we need to study how this affects the final bearing forces.

Bearing forces

Figure 10 shows polar diagrams of the bearing loads for the original compressor configuration. The red marks indicate the same angular positions as in Figure 7, taking into account the crank offsets. As mentioned before, these points coincide with the local maxima of F_t and F_r for throws two and three. For each bearing, the dotted rectangle showing the maximum forces remains the same size in subsequent polar plots, allowing easier visual comparison.

Figure 10 and Table 5 show clearly that in the original configuration, bearing three carries the highest loads. As expected, the maxima of both the horizontal and the vertical forces occur at approximately the positions of the highest pin loads on throws 2 and 3. Above all, the highest loads occur at positive values of the *x* and *y* coordinates (bottom side towards throw 1), which correlate with the observed failure pattern (Figure 4). The vertical and horizontal, as well as the resultant bearing loads of bearing three over time are shown in Figure 11. The maximum value of the resultant force is 260 kN (58,500 lbf) at the crank angle of 234 degree. This value is well above the limit of 210 kN (see section "Typical bearing failure patterns on this machine"). This fact likely contributes to the observed failures. Reducing the maximum pin forces should lead to greater reliability as a result of lower bearing loads.

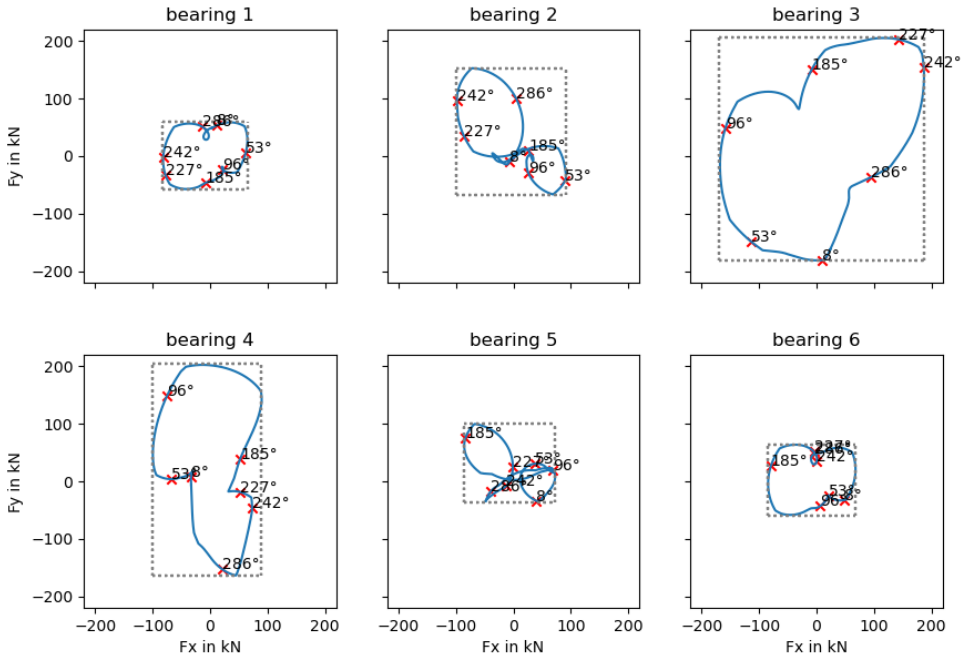

Figure 10: polar diagrams of bearing loads for the original configuration; the *y*-axis looks towards the axis of the first throw (horizontal direction), and the *x*-axis looks towards the bottom of the compressor (vertical direction).

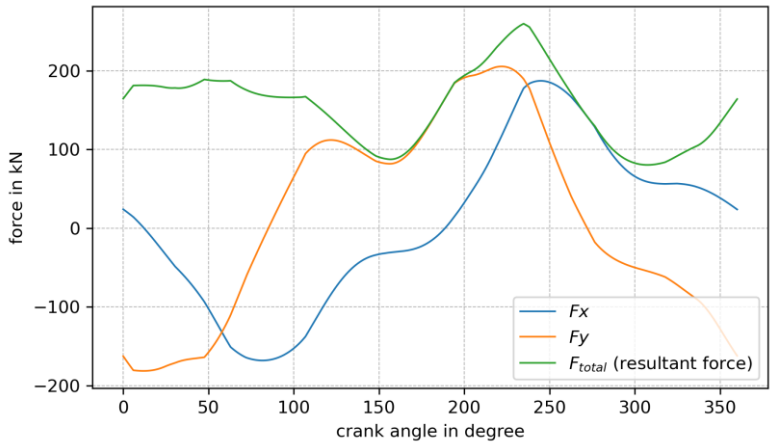

Figure 11: Horizontal forces (Fy) and vertical forces (Fx) of bearing 3.

The next step is to study how the bearing loads vary with the various proposed adjustments: lighter pistons, cylinder unloading, counterweights, and different crankshaft angles. Figure 12 (a-e) shows the polar diagrams for the various configurations and Table 5 summarizes the corresponding maxima and minima for the bearing forces.

Reducing the translational masses (Figure 12a) would reduce the maximum load by 5–14 percent. As far as the bearing loads are concerned, lighter pistons just on throws 2 and 3 would be sufficient. However, changing masses on only some of the throws would increase the free foundation forces, possibly leading to increased vibration.

Completely idling throws 2 and 3 would reduce vertical forces by up to 14 percent but would also increase the horizontal forces by up to 121 percent (Figure 12b). More promising is the 80 percent load strategy at both cylinder ends of throws 2 and 3: this configuration would reduce loads by 5–13 percent (Figure 12c).

In addition to the various configuration changes discussed above, we also studied the application of counterweights. As already mentioned, counterweights balance the rotational mass forces. They should be placed on the crank webs such that the center of gravity lies within the rotational axis. Full compensation would reduce both vertical and horizontal forces by 20–25 percent (Figure 12d) and looks like the most promising single approach to lowering the loads on bearing three.

Finally, Figure 12e shows the bearing forces considering a different crankshaft design with equal offset angles between each of the cranks (first throw at zero degree, second throw at 72 degree, third throw at 144 degree, fourth throw at 216 degree and fifth throw at 288 degree). This design would significantly lower the loads on bearing three but would significantly increase the loads on bearing four, possibly just shifting the wear problem from one bearing to the other. For that reason, this measure is not included in Table 5.

However, our best final choice is still to combine several different measures. Reducing translational masses (lighter pistons) together with the capacity approach (80 percent load on throws two and three) would reduce bearing loads by up to 24 percent. If we add counterweights, the bearing load reduction is up to 42 percent (Table 6, Figure 13 to Figure 14). The resultant maximum bearing load is reduced to 165kN: this value is well below the limit of 210kN (see section “Typical bearing failure patterns on this machine”).

Table 5: Maximum bearing forces for different configurations in kN

	Original	Lighter pistons	80% load at CE and HE of throws 2 and 3	Idle throws 2 and 3	Counterweights on throws 2 and 3
$F_{\mathrm{x,max}}$	187	175 (94%)	169 (90%)	161 (86%)	150 (80%)
$F_{\mathrm{x,min}}$	–168	–160 (95%)	–148 (88%)	–161 (96%)	–126 (75%)
$F_{y,\mathrm{max}}$	205	186 (91%)	178 (87%)	240 (117%)	171 (83%)
$F_{y,\mathrm{min}}$	–181	–156 (86%)	–172 (95%)	–220 (121%)	–138 (76%)

Table 6: Maximum bearing forces for the combination of reduced piston masses and 80 percent load at CE and HE of throws 2 and 3 in kN

	Original	Combined measures without counterweights	Combined measures with counterweights
$F_{\mathrm{x,max}}$	187	157(84%)	121 (65%)
$F_{\mathrm{x,min}}$	–168	–139 (83%)	–100 (60%)
$F_{y,\mathrm{max}}$	205	156 (76%)	123 (60%)
$F_{y,\mathrm{min}}$	–181	–148 (82%)	–105 (58%)

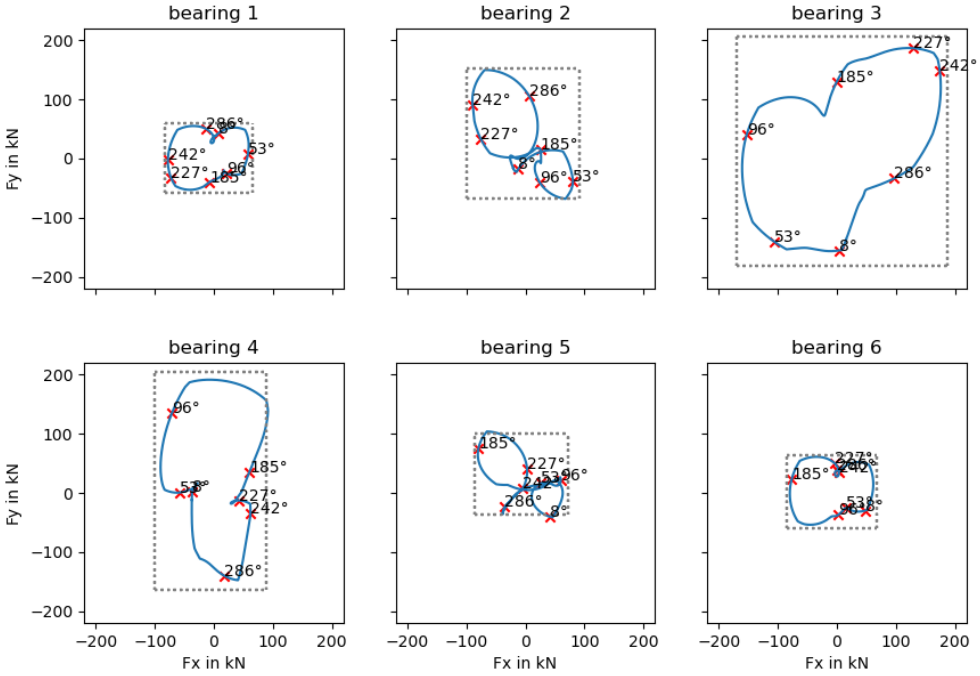

(a) Lighter pistons

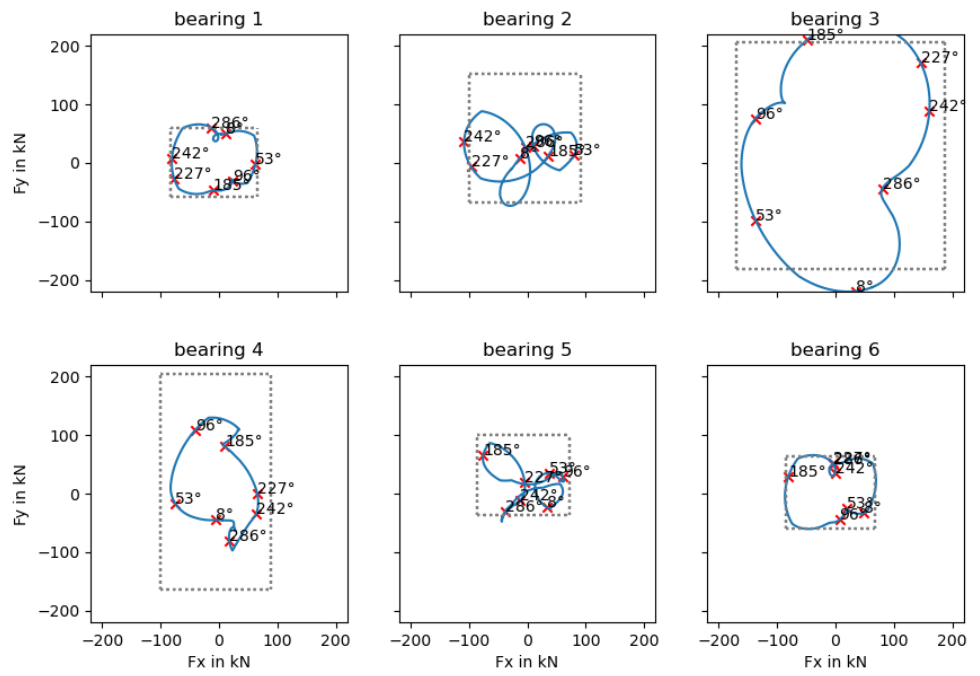

(b) Idle throws 2 and 3

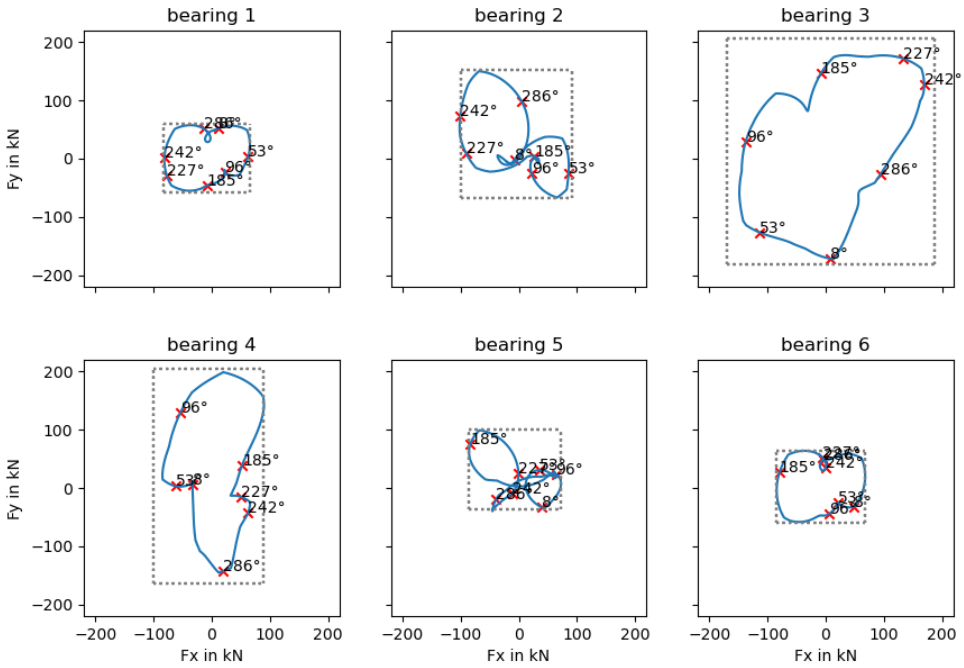

(c) 80 percent capacity at throws 2 and 3 (using stepless load capacity control system)

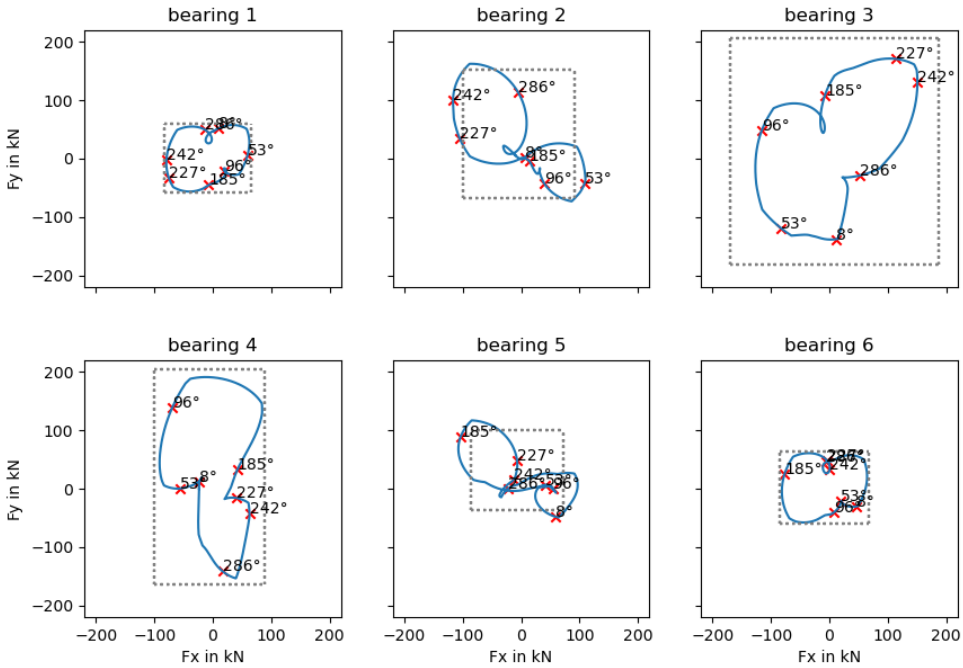

(d) Counterweights to compensate the rotating mass forces, applied to crank webs next to throws 2,3 and 4

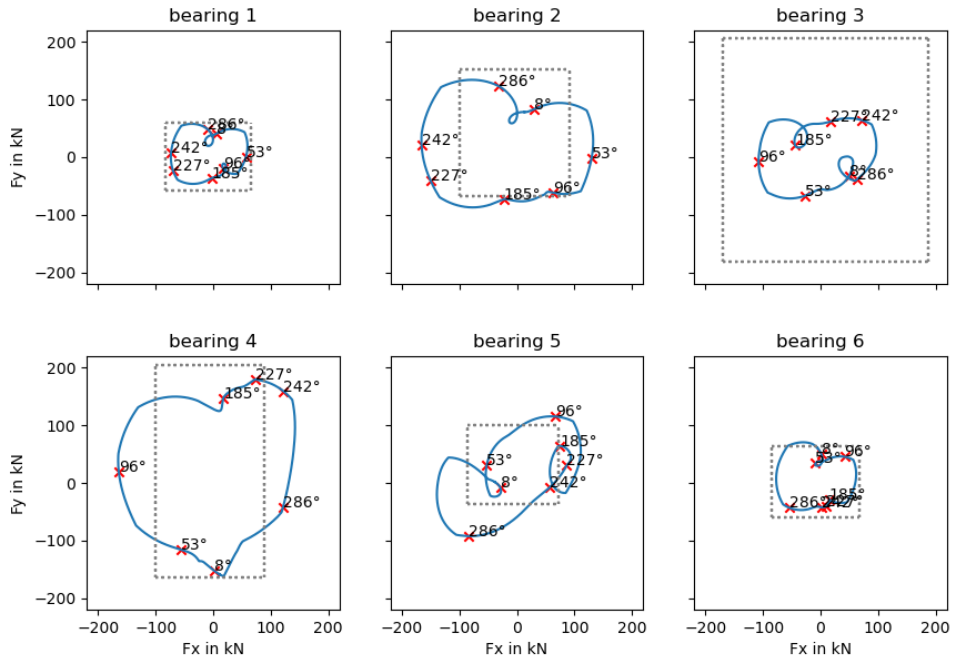

(e) Different crankshaft design with equal offset angles between all cranks

Figure 12: Polar diagrams of the bearing forces for the various system modifications studied in the previous section; the *y*-axis looks towards the axis of the first throw (horizontal direction), and the *x*-axis looks towards the bottom of the compressor (vertical direction).

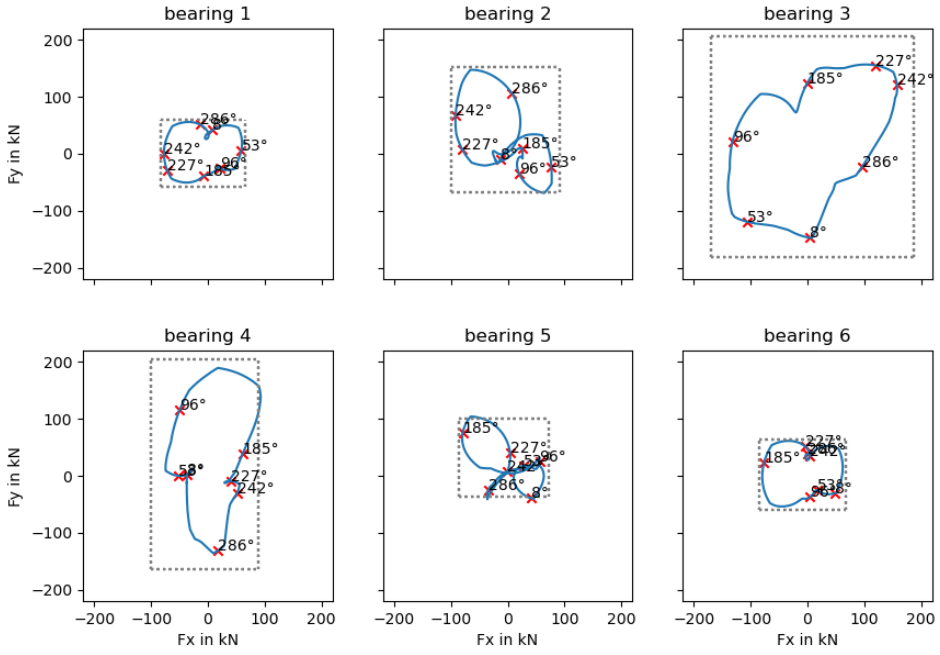

(a) Combination of 80 percent load on throws 2 and 4 with lighter pistons

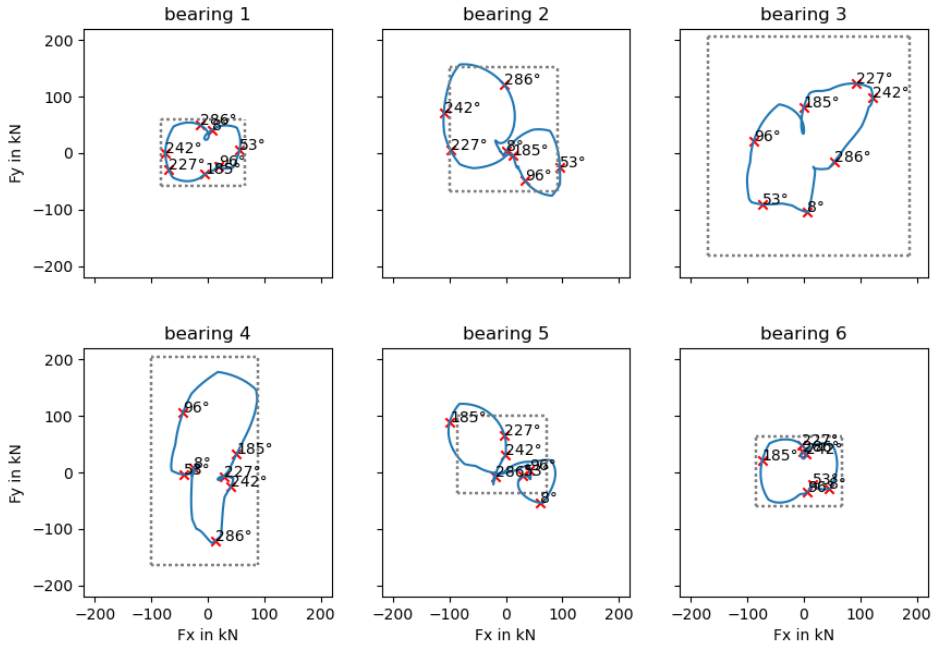

(b) Combination of 80 percent load on throws 2 and 4 with lighter pistons and counterweights next to throws 2, 3 and 4

Figure 13: Polar diagrams of the bearing forces for the combination of 80 percent load at throw 2 and 4 and decreased piston mass; the *y*-axis looks towards the axis of the first throw (horizontal direction), and the *x*-axis looks towards the bottom of the compressor (vertical direction).

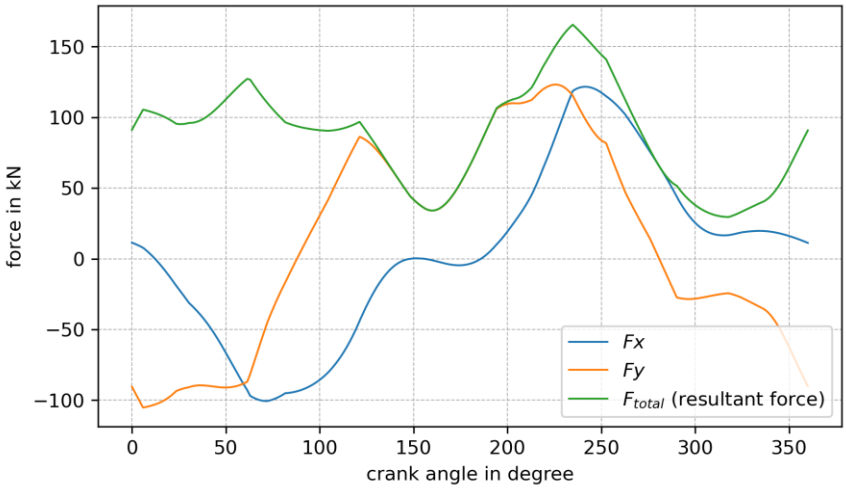

Figure 14: Horizontal forces (Fy) and vertical forces (Fx) of bearing 3, proposed design (Combination of 80 percent load on throws 2 and 4 with lighter pistons and counterweights next to throws 2, 3 and 4).

DISCUSSION AND CONCLUSION

This paper shows how a simple mechanical model can be used to estimate bearing loads effectively. The calculated regions of maximum load correlate very nicely with the failure patterns experienced in practice. The numerical model allows us to quickly compare various measures that might lower the bearing loads. Above all, the results can be used to derive new journal bearing designs.

For the specific case presented in this paper, the results suggest that a combination of three measures will be most effective. There is a clear indication that a 20 percent capacity reduction in the second and third throw, a reduction in translational masses (piston and crosshead mass), and counterweights would together reduce the load on the critical bearing no. three by approximately 40 percent, leading to a load level, which is beneath typical allowable limits found in literature for Sn-Pb alloys. These measures are in discussion with the operator and will hopefully lead to more reliable operation of this challenging group of compressors.

NOMENCLATURE

b_i	= bearing number i	(-)
φ_i	= offset angle of crank i	(-)
ρ	= influence coefficient matrix	(-)
F_{b_i}	= force acting on bearing i	(ML/T^2)
F_{c_i}	= force acting on throw i	(ML/T^2)
F_{t}	= tangential pin forces	(ML/T^2)
F_{r}	= radial pin forces	(ML/T^2)
F_i	= inertia forces	(ML/T^2)
F_{g}	= gas forces	(ML/T^2)
HE	= head end	(-)
CE	= crank end	(-)

BIBLIOGRAPHY

K.-H. Küttner, 2013, “Gemeinsame Grundlagen der Kolbenmaschinen”, Springer.

Nebojsa Nikolic, Tripo Torovic, and Zivota Antonic, 2012, “A procedure for constructing a theoretical wear diagram of IC engine crankshaft main bearings”, Mechanism and Machine Theory, 58, pp. 120–136.

Van Rossum, G., & Drake Jr, F. L.,1995, “Python reference manual”, Centrum voor Wiskunde en Informatica Amsterdam.

Herbert Wittel, Dieter Muhs, Dieter Jannasch and others, 2013, “Roloff/Matek Maschinenelemente: Normung, Berechnung, Gestaltung, Springer.